Commun Nonlinear Sci Numer Simulat 18 (2013) 81–88

Contents lists available at SciVerse ScienceDirect

Commun Nonlinear Sci Numer Simulat

journal homepage: www.elsevier.com/locate/cnsns

Non-smooth transitions in a simple city traffic model analyzed through supertracks

B.A. Toledo [a,b,*], M.A.F. Sanjuan [c], V. Muñoz [b], J. Rogan [b], J.A. Valdivia [b]

[a] Institute of Aeronautical Technology CTA/ITA/IEFM, São José dos Campos-SP 12228-900, Brazil
[b] Departamento de Física, Facultad de Ciencias, Universidad de Chile, Santiago, Chile
[c] Departamento de Física, Universidad Rey Juan Carlos, Tulipán s/n, Móstoles, Madrid 28933, Spain

ARTICLE INFO

Article history:
Received 19 December 2011
Accepted 12 June 2012
Available online 23 June 2012

Keywords:
Traffic dynamics
Supertracks
Chaos

ABSTRACT

We explore the nontrivial behavior of a particular city traffic model due to its minimalistic representation of basic city traffic dynamics. The chaotic behavior is studied through the supertrack functions, an approach that in some cases exposes more information than usual methods. In particular, we explore a parameter region that may be related to the high sensitivity of traffic flow and eventually could lead to traffic jams. First, we describe analytically a period adding region, that has a universal critical exponent of $\alpha = 1$. Second, we analyze a chaotic crisis giving rise to an inverse supertrack cascade with a period scaling of $\alpha \approx 0.49$. This cascade seems to be universal when approaching to the chaotic behavior, but in general it depends on the braking and accelerating capabilities of the vehicles.

1. Introduction

City traffic has many interesting features [1–6], some of them are of social and economical relevance [7], and display complex dynamics and emergent phenomena [8–10]. This complex behavior has been studied using many different approaches, going from statistical and cellular automaton, to hydrodynamical and mean field models [11–14]. In spite of much effort in trying to understand traffic networks, there remain many interesting problems, ranging from unexpected phenomena [15], chaotic behavior [1], self-organization [16], etc.

In this work we deepen our study of the city traffic model proposed previously in Ref. [1], which displays nontrivial dynamics and chaos, due to the finite acceleration and braking capacities of the vehicles. The appearance of chaos and nontrivial dynamics in such a minimal model of city traffic strongly suggests that chaotic behavior should be at the root of many common complex macroscopic traffic states. The nontrivial behavior in this model arises even in the non chaotic region, due to the non-smooth nature of the drivers' behavior, with well defined bounds as shown in Ref. [17]. In what follows we will denote the ratio of the minimum traveling time to the traffic light period by Ω, the minimum traveling time is the elapsed time between traffic lights at maximum speed. Therefore, the chaotic behavior that is observed for $\Omega < 1$ occurs for a range of parameters that is relevant for city traffic, through a period doubling bifurcation [1] that requires a ratio of braking and accelerating capacities greater than three. However, the nontrivial transitions such as the chaotic collision of the attractor with an upper velocity threshold which leads to a *threshold crisis* at Ωth, produce an inverse supertrack cascade for $\Omega < \Omega_{tc}$, a period doubling bifurcation for $\Omega_{tc} < \Omega < 1$, and the period adding bifurcation for $\Omega > 1$, that results when the attractor collides with the lower velocity threshold, have not been analyzed in detail. To achieve our aim of characterizing these nontrivial transitions and the chaotic behavior of the model we will make use of the supertracks functions approach

* Corresponding author at: Departamento de Física, Facultad de Ciencias, Universidad de Chile, Santiago, Chile.
E-mail address: btoledo@macul.ciencias.uchile.cl (B.A. Toledo).

1007-5704/$ - see front matter © 2012 Elsevier B.V. All rights reserved.
http://dx.doi.org/10.1016/j.cnsns.2012.06.007

(STF) [18–21]. In this approach we take a critical point of the map (a super-stable point in $\mathbb{R} \to \mathbb{R}$ maps), which in our case corresponds to a point where the gradient of the map is zero, and observe the behavior of this point as a function of a control parameter.

2. The model

The model consists of a single car traveling through a sequence of traffic lights [1]. Traffic lights can be either in green or red. The car can be in one of four possible states: (a) at rest at the position of a traffic light, (b) with constant acceleration a_+ until its velocity reaches the cruising speed $v_{\max}$, (c) with constant speed $v_{\max}$, or (d) with negative acceleration $-a_-$ until it stops or accelerates again. The dynamics may be summarized as,

$$\frac{dv}{dt} = \begin{cases} a_+\Theta(v_{\max} - v) & \text{if accelerating,} \\ -a_-\Theta(v) & \text{if braking,} \end{cases} \tag{1}$$

where Θ is the Heaviside step function.

Decisions for braking are taken at a minimum breaking distance $x_d = v_{\max}^2/(2a_-)$ of the next traffic light. If the car is at rest at a traffic light in red, it accelerates as soon as the light changes to green, until it reaches $v_{\max}$. In this model, the distance between traffic lights is always larger than $v_{\max}^2/(2a_+)$, so the car always reaches the maximum possible velocity before the next light. When the car is at a distance x_d from the next traffic light, it brakes if the light is red, and continues if it is green. If light changes from red to green before the car stops completely, the car accelerates again. With the definition taken for x_d, the car is always able to stop if it sees a red light, and if so, it is at rest in the traffic light position, until the next green light. This model generates a two dimensional map that evolves the time and speed of the car has at the nth traffic light, namely (v_n, t_n), to the time and speed of the car at the $(n+1)$th traffic light, namely (v_{n+1}, t_{n+1}).

To decide whether the nth traffic light is green or red at a given time t, the function $\sin(\omega_n t + \phi_n)$ is chosen, so that the light is green if $\sin(\omega_n t + \phi_n) > 0$ and red if $\sin(\omega_n t + \phi_n) \leqslant 0$. In the present study we will take $\omega_n = \omega = 2\pi/T$ for simplicity, where T is the period of the traffic lights. Let us also define the variable ξ_n by,

$$2\pi\,\xi_n = \omega t_n + \phi_n \bmod 2\pi,$$

which represents the signal phase. With these definitions we can construct the evolution map

$$\begin{pmatrix} v_{n+1} \\ \xi_{n+1} \end{pmatrix} = M_{\Pi}\begin{pmatrix} v_n \\ \xi_n \end{pmatrix},$$

where Π represents the parameters of the system. More details of the model, including the explicit map between consecutive traffic lights, can be found in Ref. [1].

Regarding the phase shift ϕ_n, we could introduce several control strategies as shown in Ref. [2], where we studied in some detail the case where all traffic lights are synchronized $\phi_n = 0$ and the case of a propagating green signal (green wave) for which $\Delta\phi_n = -x_n/v_{\text{wave}}$, where x_n is the position of the nth traffic light. But as was shown there, the basic dynamical features are the same. In both cases we find critical parameters values around which the dynamics changes abruptly as if the system were undergoing a phase transition. In view of this qualitative equivalence, we will restrict our study to a synchronized scenario, with $\phi_n = 0$ and $L_n = L$ where L is the distance between traffic lights. Under these conditions it is easier to follow the details, and define the critical parameter $T_c = L/v_{\max}$ and the adimensional frequency $\Omega = T_c/T$. We also define the adimensional braking and accelerating capabilities as $A_- = a_-L/v_{\max}^2$ and $a_+L/v_{\max}^2$, so $\Pi = (\Omega, A_+, A_-)$.

3. Dynamical features

In Fig. 1 we show the bifurcation diagrams associated with the dynamics described above. In this particular case we used $a_+ = 2\ \text{m/s}^2$, $a_- = 6\ \text{m/s}^2$, $v_{\max} = 14\ \text{m/s}$, and $L = 200\ \text{m}$, hence, $A_+ \approx 2.04$ and $A_- \approx 6.12$. For comparison, we also take $a_- = 10\ \text{m/s}^2$ which results in $A_- \approx 10.20$, and a second set $a_+ = 3\ \text{m/s}^2$, $a_- = 11\ \text{m/s}^2$ and $a_- = 13\ \text{m/s}^2$ which results in $A_+ \approx 3.06$, $A_- \approx 11.22$ and $A_- \approx 13.26$.

If we look at Fig. 1(a), we may believe that the system undergoes a period-2 orbit in the range $\Omega \in (1.0, 1.1)$, in which the vehicle stops at every other traffic light and goes freely in the next. However Fig. 1(b) reveals a complex pattern, as a consequence of the fact that this is a two dimensional map. A detailed study of this region [2] shows that the vehicle, after stopping at some traffic light, goes freely the next p traffic lights. We will see below that this is a period adding situation. To estimate p, we note that the driver arrives at the next signal a small time $\delta t = T_c - 2\pi/\omega > 0$ after the signal turns green. Then this delay becomes $2\delta t$ at the third light, and so on. The journey will continue until the green window is exhausted. The total number of signals, p, the driver will cross without stopping can be approximated by $p\,\delta t \approx \pi/\omega$, which leads to

$$p \approx \frac{1}{2}\frac{1}{\Omega - 1}, \tag{2}$$

from where it follows that $p \gg 1$ when $\Omega \approx 1$.

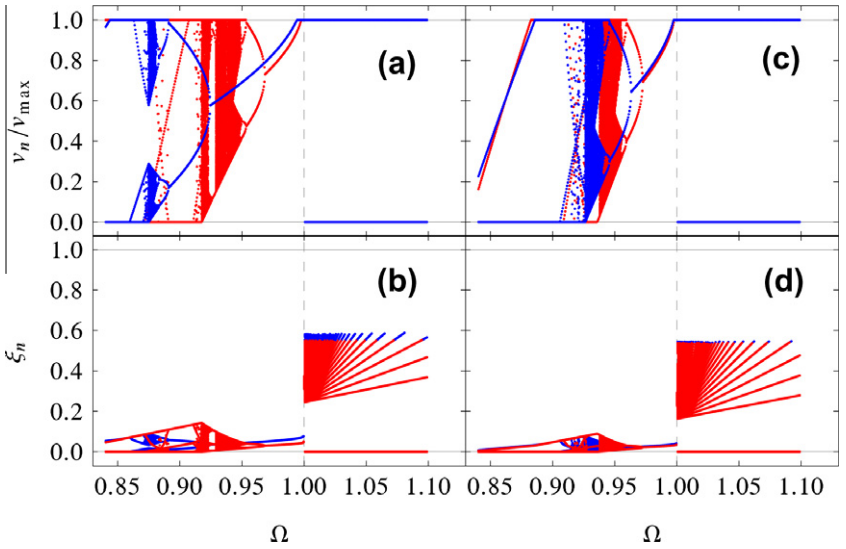

Fig. 1. Bifurcation diagrams for (a,c) the velocity at the nth traffic light and (b,d) for the phase at the nth light, for two sets of A_+ and A_-. In (a,b) we show $(A_+, A_-) \approx (2.04, 6.12)$ in blue and $(A_+, A_-) \approx (2.04, 10.20)$ in red, and in (c,d) we show $(A_+, A_-) \approx (3.06, 11.22)$ in blue and $(A_+, A_-) \approx (3.06, 13.26)$ in red. (For interpretation of the references to colour in this figure legend, the reader is referred to the web version of this article.)

Therefore, when the green light is exhausted, we reach the state $(v, \xi) = (0, 0)$ in which the car must stay with zero velocity at the traffic light until the next green light. Hence, it becomes convenient to define the supertracks functions (STF), defined by the mth iteration of the point $(v, \xi) = (0, 0)$, namely, $M_\Omega^m(0, 0)$. This STF will prove useful and help us understand the dynamics of this map. Let us note that the point $(v, \xi) = (0, 0)$ is interesting because it represents the situation in which the car is stopped completely at the traffic light, and has to wait until the next green light, which generates a periodic orbit. We also define the period of the supertracks (PST), which is defined as the smallest p integer such that $M_\Omega^p(0, 0) = (0, 0)$.

In Fig. 2 we display the normalized v component of the STFs of order 10–50 in the range (0,1), and the period p of the orbit, hence PST, as a function of Ω. This figure shows the STFs (bottom curves) associated with the velocity, from which it is immediately apparent that the dynamic is more complex than the period-2 orbit suggested by Fig. 1(a). The vertical lines occur exactly when the STF of period p transitions from $v = 0 \to 1$. The bottom curves in this figure imply a dynamics that changes progressively while the system approaches the critical point $\Omega_c = 1$, being an accumulation point. A closer examination of the asymptotic behavior of v_n, around a particular p, related to the vertical lines (which represent dynamical jumps), results in the upper curve, which is a typical period adding behavior [22], and can be found with or without chaos in many contexts [23–25]. The number $\ln(p)$ in this curve represents the number of times the vehicle arrives to the traffic light with $v_{\max}$ while approaching the critical value $\Omega_c = 1$ (at the next traffic light the vehicle is stopped and the cycle repeats). Notice, that the period can be found by counting the number of traffic lights the vehicle is able to transverse before stopping, i.e., reaches the state $(v, \xi) = (0, 0)$. The jumps in p are of one unit and correspond exactly with the changes in the STFs. This behavior arises from a time difference between the traffic light period and the travel time between consecutive

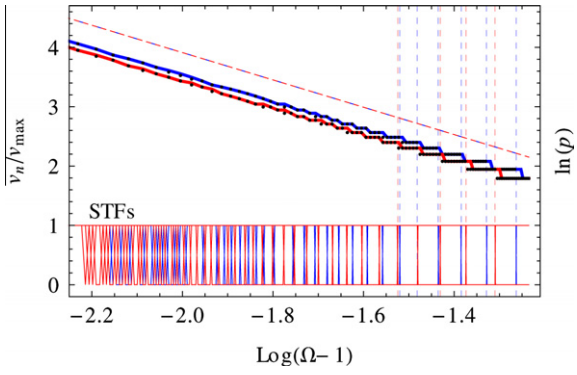

Fig. 2. Supertracks functions of order 10 to 50 associated with the velocity (bottom curves), and the period adding curve calculated numerically (dotted lines) and analytically with Eq. (5) (thick lines) and Eq. (2) (dashed lines). We also compare for $A_- \approx 6.12$ (blue) and $A_- \approx 10.20$ (red). (For interpretation of the references to colour in this figure legend, the reader is referred to the web version of this article.)

lights, and is responsible for the critical behavior observed close to $\Omega \approx 1$ [2]. Therefore, in this context, the period adding phenomenon arises from the competition between two time scales, which are, the travel time between lights (vehicle) and traffic lights period (the system with which the vehicle interacts). Following closely the periodic orbit in this region makes it possible to derive a better approximation to Eq. (2).

In the region $\overline{\Omega} > 1$, we observe a periodic motion of period much longer that T. First, let us note that the travel time between decision points when undergoing a p-period is T_c and that the mobile stops when $\sin(\omega t_p)$ changes sign from positive to negative for some p. Next, let us assume this long periodic motion can be represented by $\sin(\Lambda p + \phi)$, where $2\pi/\Lambda$ is the period of this p-oscillation, p is the number of decision points the mobile surpasses and ϕ is an initial phase. We will show below that ϕ depends on a_+ and a_- and could be relevant for small p. As shown in Fig. 3, both functions intersect providing a method for the calculation of Λ.

Note now that this p-oscillation is a solution of $\ddot{\psi} + \Lambda^2\psi = 0$. Then, solving for Λ, we obtain,

$$\Lambda = \sqrt{-\frac{\ddot{\psi}}{\psi}} \approx \sqrt{\frac{\psi_{-2} - 16\psi_{-1} + 30\psi_0 - 16\psi_1 + \psi_2}{12\psi_0}}, \tag{3}$$

where we have approximated the second order derivative $\ddot{\psi}$ by a five points finite difference. Since the traffic light signal approximates very well our p-period at t_p, we can write $\psi(t_p) \approx \sin(2\pi\Omega t_p)$. After using some trigonometric identities on Eq. (3), we obtain,

$$\Lambda \approx \sqrt{\frac{15 - 16\cos(2\pi\Omega) + \cos(4\pi\Omega)}{6}} \tag{4}$$

and find a value of p such that, $\Lambda p + \phi = \pi$. We obtain,

$$p = \left\lceil (\pi - \phi)\sqrt{\frac{6}{15 - 16\cos(2\pi\Omega) + \cos(4\pi\Omega)}} \right\rceil, \tag{5}$$

where,

$$\phi = 2\pi\left[1 + \frac{1}{2}\left(\frac{1}{A_+} - \frac{1}{A_-}\right)\right] \bmod 2\pi$$

and $\lceil \ldots \rceil$ is the ceiling function, which was included after comparing with the numerical solution, as well as our ansatz for ϕ. This function is also plotted in Fig. 2, from which we note that Eq. (5) follows with great precision the period adding behavior. Finally, let us show that the critical behavior of Eq. (5) is the same of Eq. (2) when $T \to T_c$ from the left ($\Omega > 1$). First, note that $\phi = 0$ when $a_\pm \to \pm\infty$, or equivalently, the elapsed time for braking and accelerating is negligible compared to the time travelled at a velocity $v_{\max}$ as $\Omega \to 1$. Now,

$$\begin{aligned} p &\approx \pi\sqrt{\frac{6}{15 - 16\cos(2\pi\Omega) + \cos(4\pi\Omega)}} \\ &\approx \pi\left[\frac{1}{2\pi(\Omega - 1)} + \frac{2}{45}\pi^3(\Omega - 1)^3 - \frac{1}{63}\pi^5(\Omega - 1)^5 + O\left((\Omega - 1)^7\right)\right] \\ &\approx \frac{1}{2}\frac{1}{\Omega - 1}, \end{aligned}$$

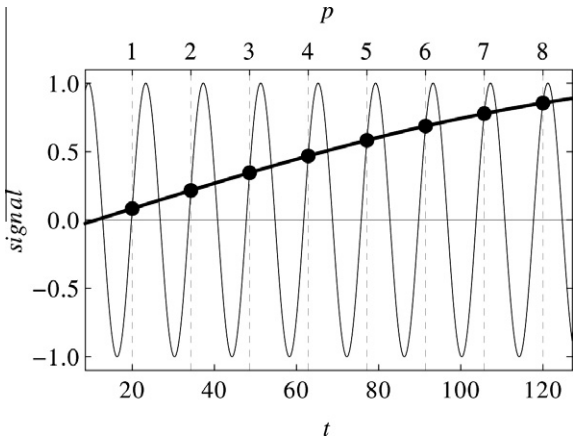

Fig. 3. Intersection points for the traffic light signal and the representation for the p-period. The thin line corresponds to the traffic light and the thick line to a p-period. Here, $\Omega \approx 1.02$. Vertical dashed lines correspond to kT_c for given $k \in \mathbb{N}$.

where we expanded in a Taylor series around $\Omega \approx 1$. We can now see that this is the result suggested by the less precise argument before Eq. (2).

In Fig. 4 we show a zoom of Fig. 1(a) for $\Omega < 1$, and we can see a crisis around $\Omega_{tc} \approx 0.875$ for $A_- \approx 6.12$, where the chaotic attractor collides with the state $(v, \xi) = (0, 0)$ as we decrease Ω, which means that the mobile needs to wait until the next green light. This is not a boundary crisis as the attractor is not able to go to another basin, due to the restriction $v \geqslant 0$. Furthermore, the STFs seem to follow the asymptotic behavior of the dynamics, which means that for a given set of parameters, we could write explicit polynomials in Ω that will follow analytically the asymptotic behavior of the mobile in this region, i.e., for $\Omega < \Omega_{tc}$ the asymptotic dynamics is bounded by the STFs, with the dynamics of stop-and-wait described above. Note that this behavior is different to the case $\Omega > 1$. This figure also suggests an interesting relation between chaos with the spread and slope of STFs. Note that the STFs with high slope are associated with complex dynamics, in this way the derivative of STFs may be used to search for non trivial dynamics in a two dimensional map. This suggestion is enforced by Fig. 5, where we compare a region of complex behavior with a set of STFs. As is readily apparent there is a close correlation between high slope STFs and a complicated motion. The closely packed STFs, corresponding to almost vertical lines in Fig. 5(b), are similar to those related to the period adding phenomena in Fig. 2, for which a jump is associated with a drastic dynamical change. The difference in the pre-crisis region is its frequency. In the period adding region, the discontinuities in STFs are isolated events as described approximately by Eq. (5), however, in this pre-crisis dynamics we see the emergence of regions where STFs with high slope accumulate, giving rise to a highly unstable dynamics due to very frequent (possibly continuous) and drastic dynamical changes. However, these orbits are not chaotic in the asymptotic sense, as we will show next, giving rise to a new complex dynamics as far as we know. Therefore, since STFs delimit the regions where orbits exist, sudden changes in these boundaries make the orbits very complex, without chaos.

For $\Omega < \Omega_{tc} \approx 0.875$ (for $A_- \approx 6.12$) we see a particular non chaotic orbit of large period p, that can be characterized by the given STFs. Hence, we have a periodic orbit that starts at $(v, \xi) = (0, 0)$ and returns to the same state after p iterations. It is important to mention that if we were trying to calculate a numerical Lyapunov exponent, we could obtain a positive value when the p is large, however the orbit is periodic. It is interesting to note that the transition from the chaotic behavior to these periodic orbits seems to occur continuously in the following sense.

In Fig. 6(a) we show the length of the periodic orbits $\Omega < \Omega_{tc}$ in the range $\Omega \in (0.8748, 0.8750)$, which is equivalent to the period of the supertracks (PST), as we approach Ω_{tc}. This calculation can be done by starting at $(t_0, v_0) = (0, 0)$ and counting the iterations it takes to return to the same state. If we repeat this analysis in the chaotic region we will obtain, of course, an infinite PST, which provides a method to determine Ω_{tc} with a large enough accuracy. We observe an inverse supertrack cascade, in which the PST has a scaling that goes as

$$\mathrm{PST} \sim |\Omega - \Omega_{tc}|^{-\alpha}.$$

In the case of $A_- \approx 6.12$, shown in Fig. 6(a), the scaling is $\alpha \approx 0.47$. The same analysis is repeated for $A_- \approx 10.20$ in Fig. 6(b), giving a scaling described by the index $\alpha \approx 0.50$. Hence, this cascade seems to be universal very close to Ωth, however, it depends on the braking and accelerating capabilities of the vehicles much farther. It is important to note that this non trivial behavior is not completely equivalent to that found in the period adding region, although, both are possible due to the imposed thresholds that produce the super-stable point $(v, \xi) = (0, 0)$.

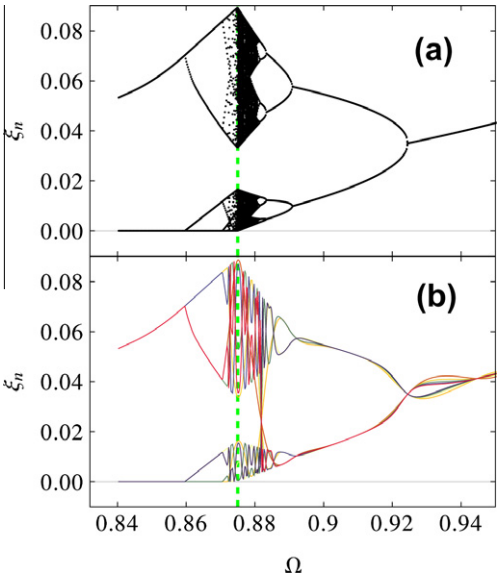

Fig. 4. Bifurcation diagrams for the signal phase at the nth light, with some of their associated STFs (from order 7th to 15th, color online). In (a) the attractor image and (b) the STFs. The thick dashed line corresponds to $\Omega_{tc} \approx 0.875$.

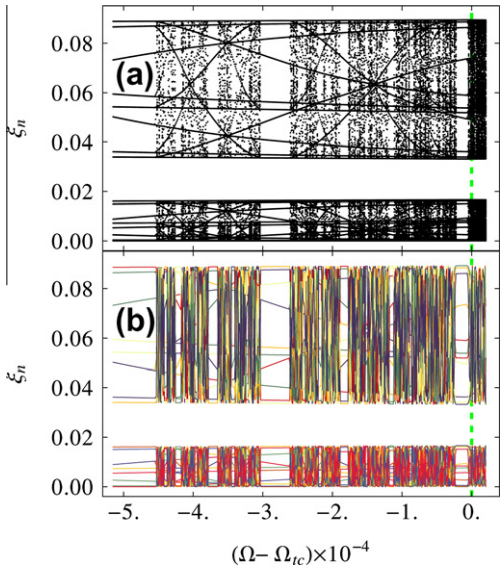

Fig. 5. Pre-crisis dynamics. (a) The attractors for $\Omega < \Omega_{tc}$ and (b) the associated STFs of order 30 to 58. The dashed line corresponds to Ω_{tc}.

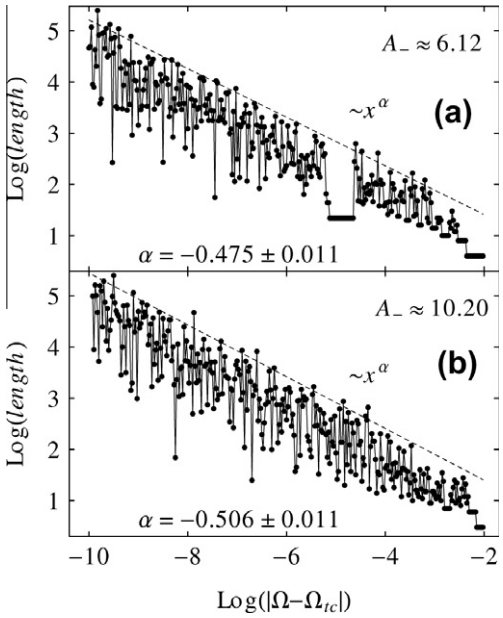

Fig. 6. Length of the orbit, represented by the number of traffic lights between full stops. Note the seemingly random pattern and the overall scaling behavior.

We can now see that the STFs provide us with an understanding of the origin of this chaotic crisis, and the behavior before and after that. This transition is a consequence of the rules the drivers must follow and that are included in this model, as represented by the threshold values. When the chaotic attractor collides with the state $(v, \xi) = (0, 0)$, it produces an inverse supertrack cascade in which the period of the supertracks decreases with distance from the crisis. Note also that this crisis is not a standard boundary crisis, nor a standard internal crisis, nor a chaotic merging crisis. For $\Omega > \Omega_{tc}$, in the chaotic attractor, there is a clear intermittency close to the STFs, which survives into the chaotic attractor, as shown in Fig. 7. It seems as if we were unraveling the periodic orbits of a non-attracting chaotic set (inside the chaotic attractor) as we decrease Ω from Ω_{tc}.

As an illustration, in Fig. 7(a) we show the region where the crisis occurs and two colliding STFs of orders 1 and 23. Of course STFs of higher order also collide in this range. Since STFs are boundaries for chaotic motion, the tangent collision, force

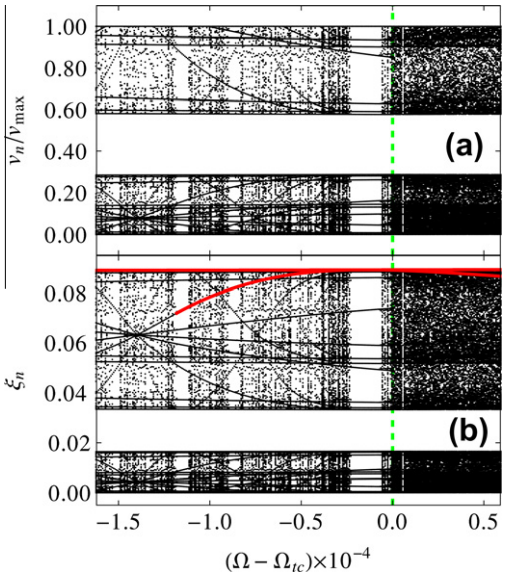

Fig. 7. Bifurcation diagram that clearly shows the intermittent behavior close to the STFs, which are projected into the chaotic regime $\Omega > \Omega_{tc}$.

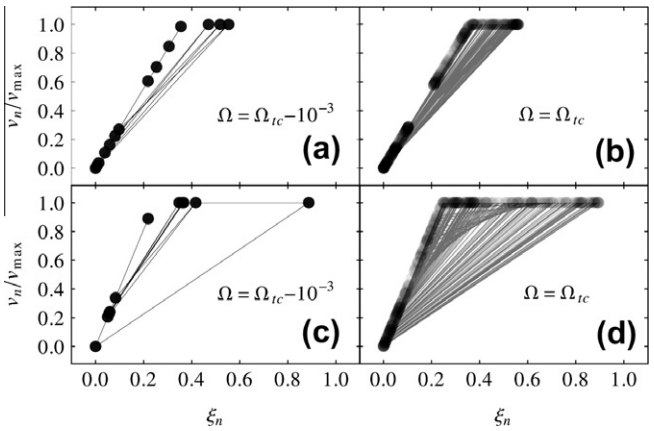

Fig. 8. Phase portrait (v, ξ) of 2 trajectories for $A_{-} \approx 6.12$, (a,b) and $A_{-} \approx 10.20$, (c,d). In (b) and (d) we show a trajectory in the chaotic attractor. For each figure we plot 500 trajectory points and the lines connecting them give an idea of the path followed. The orbit length in (a) is 14 and in (c) 13.

a collapse in the phase space, generating the conditions for the first full stop (Fig. 7(b)). The collision shown in Fig. 7(b) is responsible for the largest periodic window in the figure, which has period 22.

Finally, in Fig. 8 we show the phase portrait in (v, ξ) space, of these periodic trajectories that appear for $\Omega < \Omega_{tc}$, as we approach Ω_{tc}. This is done for two values of the braking capability, $A_{-} \approx 6.12$ and $A_{-} \approx 10.20$. For both of them, we have taken a sample path of 500 orbit points. In this figure we note the increased range for ξ_n when $A_{-} \approx 10.20$, which is consistent with the enlarged chaotic attractor found for this parameter and illustrates how these orbits go from a periodic behavior to a chaotic one as suggested by Fig. 6. We can see that these long periodic orbits were unstable periodic orbits that were part of the chaotic attractors and now are forced to a stable periodic behavior by the thresholds.

4. Conclusions

Although STFs are not widely used, they can provide interesting information about the dynamics, specially for non-smooth maps like the city traffic model we have analyzed in this manuscript. In our map, the STFs represent periodic orbits that can describe the asymptotic behavior during the period adding bifurcation that appears for $\Omega > 1$, and before the chaotic crisis for $\Omega < \Omega_{tc}$. We can observe a very complicated behavior that can be described by an inverse supertrack cascade represented by a divergent length of the periodic orbits as we approach $\Omega \to \Omega_{tc}$, in which case the orbit period becomes infinite,

and we enter into the chaotic attractor generated by the period doubling bifurcation as Ω decreases from $\Omega = 1$. This transition is a consequence of the rules the drivers must follow and that are included in this model, as represented by the threshold values. It is not one of the standard crisis (e.g., boundary, internal, or chaos merging), and as such, it deserves further attention, which will be done elsewhere.

Acknowledgments

This project has been financially supported by FAPESP (BAT), and FONDECyT under contracts No. 1110135 (JAV), No. 1090225 (JR) and No. 1080658 (VM). We also thank CEDENNA and a CNPq-Conicyt Grant. Financial support from the Spanish Ministry of Science and Innovation under Project No. FIS2009-09898 (MAFS) is also acknowledged.

References

[1] Toledo BA, Muñoz V, Rogan J, Tenreiro C, Valdivia Juan Alejandro. Modeling traffic through a sequence of traffic lights. Phys Rev E 2004;70(1):016107.
[2] Toledo BA, Cerda E, Rogan J, Muñoz V, Tenreiro C, Zarama R, et al. Universal and nonuniversal features in a model of city traffic. Phys Rev E 2007;75:026108.
[3] Wastavino LA, Toledo BA, Rogan J, Zarama R, Muñoz V, Valdivia JA. Modeling traffic on crossroads. Physica A 2007;381:411–9.
[4] Nagatani Takashi. The physics of traffic jams. Rep Prog Phys 2002;65(9):1331–86.
[5] Nagatani Takashi. Clustering and maximal flow in vehicular traffic through a sequence of traffic lights. Physica A 2007;377(2):651–60.
[6] Lämmer Stefan, Helbing Dirk. Self-control of traffic lights and vehicle flows in urban road networks. J Stat Mech 2008:04019.
[7] Helbing Dirk, Treiber Martin. Jams, waves, and clusters. Science 1998;282:2001–3.
[8] Bar-Yam Y. Dynamics of complex systems. Addison-Wesley; 1997.
[9] Bar-Yam Y. Unifying themes in complex systems. New England complex systems institute series on complexity. Westview Press; 2003.
[10] Nicolis Gregoire, Prigogine Ilya. Exploring complexity: an introduction. W.H. Freeman & Company; 1989.
[11] Lee HK, Lee H-W, Kim D. Macroscopic traffic models from microscopic car-following models. Phys Rev E 2001;64(5):056126.
[12] Matsukidaira Junta, Nishinari Katsuhiro. Euler–Lagrange correspondence of cellular automaton for traffic-flow models. Phys Rev Lett 2003;90(8):088701.
[13] Mitarai Namiko, Nakanishi Hiizu. Spatiotemporal structure of traffic flow in a system with an open boundary. Phys Rev Lett 2000;85(8):1766–9.
[14] Nishinari Katsuhiro, Treiber Martin, Helbing Dirk. Interpreting the wide scattering of synchronized traffic data by time gap statistics. Phys Rev E 2003;68(6):067101.
[15] Lee Hyun Keun, Barlovic Robert, Schreckenberg Michael, Kim Doochul. Mechanical restriction versus human overreaction triggering congested traffic states. Phys Rev Lett 2004;92(23):238702.
[16] Tadaki S, Kikuchi M, Nakayama A, Nishinari K, Shibata A, Sugiyama Y, et al. Power-law fluctuation in expressway traffic flow: detrended fluctuation analysis. J Phys Soc Jpn 2006;75(3):034002.
[17] Villalobos J, Toledo BA, Pastén D, Muñoz V, Rogan J, Zarama R, et al. Characterization of the nontrivial and chaotic behavior that occurs in a simple city traffic model. Chaos 2010;20:0131109.
[18] Oblow EM. Supertracks, supertrack functions and chaos in the quadratic map. Phys Lett A 1988;128:406.
[19] Barabási AL, Nitsch L, Dorobantu IA. Supertracks and *n*th order windows in the chaotic regime. Phys Lett A 1989;139(1–2):53–6.
[20] Barabási A-L, Nitsch L, Dorobantu IA. On crises and supertracks: an attempt of a unified theory. Rev Roumanie Phys 1989;34:353–7.
[21] Leo M, Leo RA. Supertrack functions in one-dimensional maps. II Nuovo Cimento B 1993;109(3):229–38.
[22] Van Der Pol Balth, Van Der Mark J. Frequency demultiplication. Nature 1927;120:363–4.
[23] Fan Yin-Shui, Chay Teresa Ree. Generation of periodic and chaotic bursting in an excitable cell model. Biol Cybern 1994;71(5):417–31.
[24] Sanjuan Miguel AF. Symmetry-restoring crises, period-adding and chaotic transitions in the cubic van der pol oscillator. J Sound Vib 1996;193(4):863–75.
[25] Che Yan-Qiu, Wang Jiang, Si Wen-Jie, Fei Xiang-Yang. Phase-locking and chaos in a silent hodgkin–huxley neuron exposed to sinusoidal electric field. Chaos Solitons Fract 2009;39(1):454–62.